Correlation of Material Properties and Machine Learning Techniques on a TIG Cladded SS 316L Base Alloy with SS 304 Filler

Varun Kumar A.
Assistant Professor (Sr.Gr)
Department of Mechanical Engineering
B S Abdur Rahman Crescent Institute of Science and Technology, Vandalur
Chennai-48
India

Shanmuga Vadivu K.R.
Assistant Professor
Department of Electrical and Electronics
B S Abdur Rahman Crescent Institute of Science and Technology, Vandalur
Chennai-48
India

Sathickbasha K.
Assistant Professor (Sr.Gr)
Department of Mechanical Engineering
B S Abdur Rahman Crescent Institute of Science and Technology, Vandalur
Chennai-48
India

Tungsten Inert Gas (TIG) cladding is the most promising and feasible technique adopted for the weldability of stainless-steel alloys. In this work, SS 304 fillers were deposited over the SS 316L through the TIG cladding process, and the alloy behavior was studied. The optical study, tensile, and microhardness values of TIG-cladded SS 316L base metal with the SS 304 filler material correlate with the machine learning technique. The Adaptive Neuro-Fuzzy Inference Systems (ANFIS) model is utilized in this study to predict the values theoretically. The correlation between the experimental values and theoretical values is shown to be in good agreement. The enhancement in the mechanical properties of TIG-cladded SS 316L alloy is found to be sounder and more reliable than that of the SS 316L base alloy. The suitable selection of process parameters and the type of cladding (single or double pass) had a significant effect on the improvement of material properties to a greater extent. From the experimental results, the increase in the tensile and microhardness values was found to be 13.2 % and 42.5 %. However, a wide range of methodologies/techniques are available for the theoretical prediction of values, whereas the machine learning technique had a significant effect on the reliable prediction of values. Therefore, it is found that the adoption of machine learning techniques can help flexibly for the identification of a reliable and optimal process parameter in a fabrication process.

Keywords: *TIG cladding, SS 316L, SS 304 Filler, Material Properties, Machine Learning Technique, and Optimal process parameter prediction.*

1. INTRODUCTION

Austenitic stainless steels, especially 300 series, contain sufficient chromium and nickel to maintain the austenite phase in the room-temperature atmosphere. Due to the chromium content, the corrosion resistance is at a higher level, and they are widely used in industries such as heat exchangers, furnaces, turbines, and vessels [1]. It is reported [2-4] that austenitic stainless steels are prone to high thermal expansion and reduced thermal conduc–tivity. Thus, these characteristics of austenitic stainless steel create huge challenges during the solidification process. The austenitic stainless steel is subject to hot cracking during welding due to the absence of ferrite contents [5]. Another major complexity with austenitic stainless steel is solidification cracking, and necessary care must be taken to prevent this defect. The AISI 300 series solidifies in the welding process as a mixture of austenite and ferrite. Few research works have been reported on the cladding of a substrate over austenite stainless steel alloys for better corrosion resistance [6-8]. Limited research work was reported towards the enhancement of material properties with the assistance of the cladding process. It has been reported that the process parameters play a vital role in the weldment's material properties [9-13]. Thus, it is necessary to have control over the process parameters to get a reliable sound bonding of the material. In this scenario, machine learning plays a major role in determining the optimal parameters. It helps define reliable process parameters more easily than other conventional methods. A variety of non-linear methods are being adopted, such as the Taguchi method [14–17], response surface method [18–22], artificial neural network (ANN) [23–26], genetic algorithm [27], and the particle swarm optimization techniques [28–30] have been predominantly used to represent the relationship between the process parameter and the respective outputs from the weldments. Few research works have been reported on quality evaluation, distortion control, and mechanical property investigations [31-33]. It is found that the major part has been contributed by the process parameter and the process chosen for bonding. However, appropriate optimization techniques can be adopted for reliable and sound joints between the alloys.

The existing conventional methods for process para–meter optimization (Taguchi approach, Grey relational analysis, etc.) require time to determine the values thr–ough mathematical calculations. In contrast, in machine learning techniques, the procured time is less, and we can also relate the fabrication process with multiple process parameters, which is practically very tedious

Received: October 2024, Accepted: December 2024
Correspondence to: Dr. Sathickbasha K,
B S Abdur Rahman Crescent Institute of Science and Technology, Vandalur, Chennai- 48, India.
E-mail: sathick.basha@crescent.education
doi: 10.5937/fme2501113K

with conventional methods. The machine learning techniques are also very flexible in case we need to change the process parameters, and we can identify the optimal process parameter for the same. Thus, the flexibility that exists in machine learning techniques is inevitable, which makes it superior for the employment of a system for the efficient prediction of values and reliable process parameters. Among the conventional methods, machine learning techniques have a significant effect in defining the optimal process parameters. The major objective of this work is to relate the material property with the machine learning technique. This approach is inevitable in mass production systems where we can predict the reliable process parameter or the working range of parameters in a process. This methodology considerably reduces the time factor needed to identify a reliable and feasible range of process parameters efficiently. The flexibility of adop–ting the machine learning technique in a manufacturing process will be an added advantage for the production engineer, which will help reduce the time factor to a greater level when compared with other traditional methodologies. The core application of employing machine learning techniques is to enhance the efficiency in a mass production system where the process para–meters utilized are in higher numbers. However, no evident work has been performed on the material property of a TIG-cladded SS 316L alloy with the SS 304 filler and machine learning technique. Therefore, in this study, we have correlated the effectiveness of adop–ting machine learning techniques to identify the optimal process parameters concerning the material properties of the cladded alloy. It is revealed that the predicted values of tensile, microhardness, and optical analysis of the samples are found to be in line with the experimental data. Thus, machine learning techniques can be significantly utilized for the theoretical prediction of values and to determine the optimal process parameters.

2. ARTIFICIAL NEURAL NETWORK (ANN)

Artificial Neural Network (ANN) is a decision tree model-like structure that uses different input parameters to get the required output as per the requirement or application. It carries a three-layer structure in general. However, the layers are to be categorized based on the problem we have in the system. The ANN serves as a simplified model of the Biological Neural Network (BNN). It processes interconnected signals from a sys–tem that includes high-speed signal transportation, information storage, perception, automatic training, and modeling. In the ANN, inputs (X) are assigned weight percentages (W) and summed in a summation unit, represented as [(X1 x W1) + … + (Xn x Wn)]. These signals then proceed to a threshold unit, or transfer function (Φ), which determines whether the signals exceed a certain threshold. If they do, they are passed to the output; otherwise, they are discarded. Common types of transfer functions in ANNs include hard-limit, linear, and sigmoid functions. The ANN architecture comprises three layers: an input layer for initial parameters, a hidden layer for processing, and an output layer for results. ANNs offer superior mapping capa–bilities compared to traditional methods, making them ideal for complex mathematical modeling. The first ANN model was implemented in the GTAW process [34].

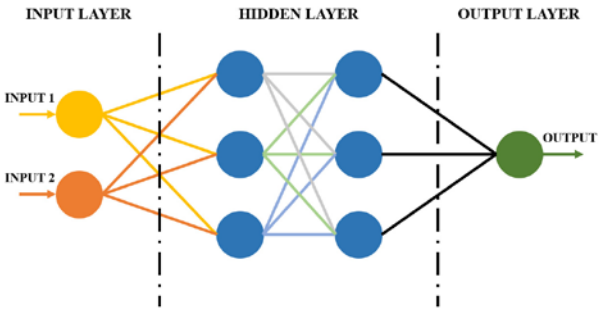

Figure 1. Schematic representation of ANN with two input variables

An enhanced ANN and neural network model were developed for predicting and selecting various welding processes [35-38]. Different algorithms can be emp–loyed with the ANN based on specific applications, with popular options including back-propagation, counter-propagation, and genetic algorithms. These algorithms are widely used in ANN models due to their superior performance compared to others. It is important to note that the material joining process is significantly influen–ced by process parameters, regardless of the type of welding method used. Figure 1 shows the schematic view of the ANN model with a three-layer structure.

3. ADAPTIVE NEURO-FUZZY INFERENCE SYSTEM (ANFIS)

The ANFIS model carries a different layer of structures in its system. However, the number of layers in the ANFIS model can be varied or modified based on the requirement. Meanwhile, it is always advised to have a wide number of layers and more parameters during the model development. A larger number of process para–meters is always likely to provide a better accuracy va–lue with the least error percentage in the model. Takagi and Sugeno's approach, known as ANFIS, was deve–loped in early 1993 and has since gained widespread application due to its efficiency and accuracy compared to other neural network models. In the ANFIS frame–work, inputs are typically treated as a linear distribution, although non-linear distributions can also enhance accuracy. The outputs are functions of these inputs, which are represented by membership distribution functions characterized by three linguistic terms. During model training, varying the parameters \(d1\) and \(d2\) (representing the length of the distribution function) helps achieve modified distributions for the inputs. The ANFIS model comprises six layers: Layer 1 (Inputs), Layer 2 (Fuzzification), Layer 3 (Firing Strength Values), Layer 4 (Normalized Firing Strength Values), Layer 5 (Outputs calculated as the product of norma–lized firing strength values), and Layer 6 (Overall Out–put). Each layer plays a crucial role in training and model development. As depicted in Figure 2, the archi–tecture includes notations for circles and squares, where the squared variables indicate the potential for further

optimization to enhance accuracy. This optimization can involve error minimization algorithms using input variable coefficients (\(ai\), \(bi\), and \(ci\)). When a Genetic Algorithm is employed for this purpose, it is referred to as the ANFIS model. Overall, ANFIS offers a robust solution for theoretical value predictions.

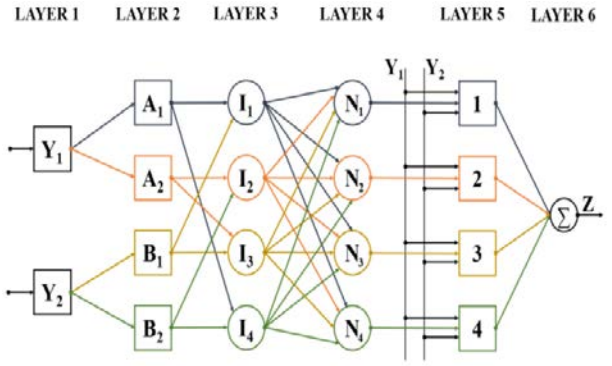

Figure 2. ANFIS Architecture

4. EXPERIMENTAL DETAILS

SS 316L (5 mm) plate dimensions used in this research can be observed in Figure 3 and SS 304 filler wire of around 1.8 mm diameter. The SS 316L and SS 304 filler were procured from Bishweshwar Steels, India. The respective chemical compositions are listed in Table 1. Among the several grades of austenitic stainless steel, SS 316L and SS 304 were obtained for this study to investigate the material's behavior throughout the cladding process.

Table 1: SS 316L and SS 304 chemical composition in weight (%)

Elements	SS316L	SS304
	Wt%	
C	0.03	0.04
Si	1	0.44
Mn	2	1.4
P	0.045	0.03
S	0.016	0.02
Cr	17.4	17.8
Ni	12.6	9.4
N	0.14	0.1
Mo	2.14	-
Fe	Balance	Balance

The procured samples were properly wire brushed, and ethanol was utilized to remove dirt from the alloy surface. The fabricated samples are properly polished with emery-grade sheets and etched for the optical study. The samples for the optical, microhardness, and tensile tests are fabricated through the wire-cut EDM process for a better surface finish. Meanwhile, the wire-cut EDM process doesn't affect the base material properties due to their less heat generation during the cutting process than other conventional fabrication processes. The tensile samples are fabricated as per the ASTM standard (E8M-04). Figures 4 and 5 depict the representation of the sample for the optical, micro–hardness, and tensile tests. Figure 6 denotes the sche–matic representation of the tensile specimen ASTM standard. The process parameters used in this study are listed in Table 2. For the theoretical prediction of mechanical properties (ANFIS), an approach is adopted, and the same is correlated with the experimental values.

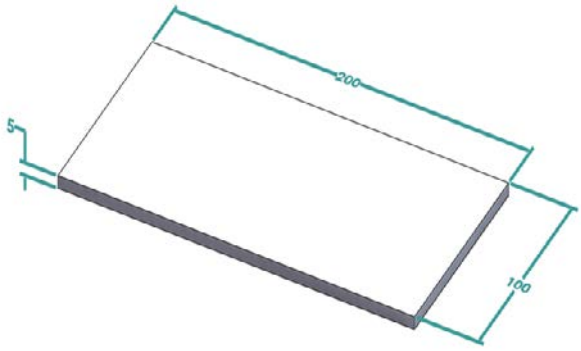

Figure 3: Schematic representation of plate

Figure 4: Optical and Microhardness sample [42]

Figure 5: Tensile sample [42]

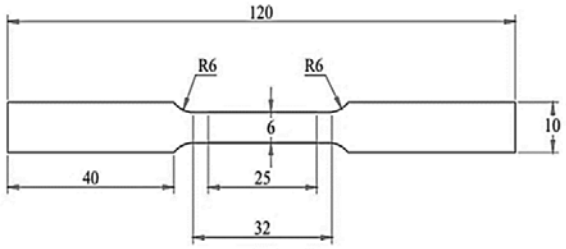

Figure 6: ASTM E8M-04

Table 2: Process parameters

S. No	Current [amp]	Flow rate [lpm]	Travel Speed (mm/sec)	Number of Passes
Sample 1	80	0.5	2	Single Pass
Sample 2	90	1.0	4	Single Pass
Sample 3	100	1.5	6	Single Pass
Sample 4	110	2.0	8	Single Pass
Sample 5	120	2.5	10	Single Pass
Sample 6	80	0.5	2	Double Pass
Sample 7	90	1.0	4	Double Pass
Sample 8	100	1.5	6	Double Pass
Sample 9	110	2.0	8	Double Pass
Sample 10	120	2.5	10	Double Pass

5. MATERIAL CHARACTERIZATION AND MECHA–NICAL PROPERTIES

The optical analysis is carried out for the cladded samples across the cross-section. The different regions

of the cladded samples were identified in the analysis (clad region, base alloy, zone separation). Figures 7 and 8 depict the optical and SEM images for sample number 6; among the wide number of trials performed, we have critically taken sample number 6 for the correlation of the metallurgical and mechanical properties. Sample 6 was chosen for the discussion based on the enhanced metallurgical properties and superior mechanical pro–perties compared with the other trials performed in this study. From the optical study, it is revealed that the pre–sence of ferrite contents in the clad zone is due to the deposition of the SS 304 filler wire. The transformation of the austenite to ferrite is due to the temperature factor involved in the process. However, the transformation of this property in the stainless steel determines the metal–lurgical property of the alloy in a process. Meanwhile, the transformation of this phase can happen naturally, or it can also be performed by adopting rapid cooling of the temperature after the fabrication process. However, the rapid cooling of the alloy will also have a subtle effect on the material property, such that a rapid cooling process can be followed based on the need and requi–rement of a problem.

The conversion of the austenite (γ) to ferrite (δ) or the combination of both in the material can happen in the base alloy is purely dependent on the temperature variations that occur during or after the process. The transformation of the (γ to δ) is evident from the micrograph with the primary solidification of the (γ) as reported [39]. The phase transformation is due to the thermal dissipation in the process, and it can be controlled by adopting reliable process parameters. It is reported [40] that the variation of phases primarily influences the changes in the material property due to the heat generated in the process.

As our base substrate is SS 316L which is being de–posited or cladded with the SS 304 filler. Sample 6 proved to have a refined grain structure due to the utili–zation of reliable process parameters and adoption of the double pass cladding which helped in depositing a reasonable quantity of SS 304 filler over the base alloy.

Table 3: Experimental tensile test values

S. No	Current [A]	Flow Rate [LPM]	Travel Speed (mm/sec)	UTS (MPa)
Sample 1	80	0.5	2	495.8
Sample 2	90	0.5	4	544.16
Sample 3	100	1.0	6	527.37
Sample 4	110	1.5	8	477.58
Sample 5	120	2.0	10	479.41
Sample 6	80	0.5	2	582.5
Sample 7	90	0.5	4	577.15
Sample 8	100	1.0	6	551.25
Sample 9	110	1.5	8	505.67
Sample 10	120	2.0	10	576.74

It is always evident that (δ – Fe) content and improved grain boundary structures will always have a good impact on the other mechanical properties. In this study, we have considered tensile and microhardness as properties related to metallurgical properties due to the fact that these two properties predominantly define the strength of the alloys. The observed tensile and microhardness values for the process parameters are listed in Tables 3 and 4. The base alloy without cladding has an ultimate tensile value of ≈ 520 MPa and microhardness of ≈ 160 Hv. The cladded base alloy SS 316L with the SS 304 filler has shown improved tensile and microhardness values. The improved efficiency was observed in a 13.2 % increase for the tensile and a 42.5 % increase in the microhardness [42]. Further, the enhanced mechanical properties align with the alloy's metallurgical behavior; in addition, the process para–meters also play a major role in deciding the material properties. It is reported that the pure solidification of SS 304 filler over the base substrate has significantly improved the grain structures and enhanced the mec–hanical properties to a greater extent [42].

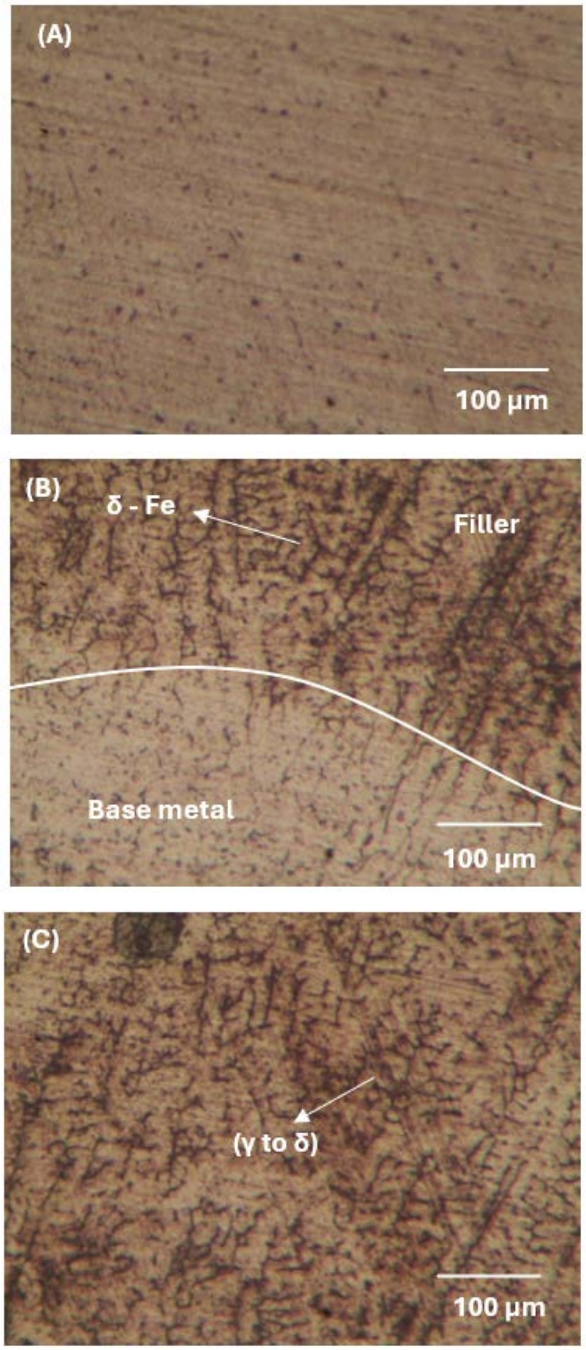

Figure 7: Sample 6 - Optical micrograph, (A) – Base alloy, (B) – Fusion zone between base alloy and filler, (C) – Filler region [42]

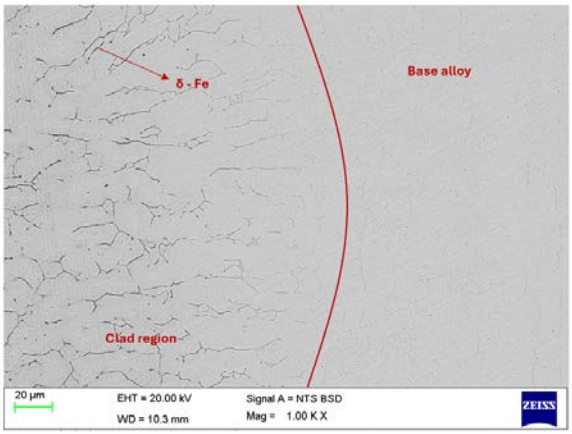

Figure 8: Sample 6 SEM micrograph [42]

Table 4: Experimental microhardness values

S. No	Current [A]	Flow Rate [LPM]	Travel Speed (mm/sec)	Microhardness (Hv)
Sample 1	80	0.5	2	207.2
Sample 2	90	0.5	4	216.3
Sample 3	100	1.0	6	203.3
Sample 4	110	1.5	8	200.8
Sample 5	120	2.0	10	189.6
Sample 6	80	0.5	2	220.5
Sample 7	90	0.5	4	204.6
Sample 8	100	1.0	6	209.4
Sample 9	110	1.5	8	214.1
Sample 10	120	2.0	10	210.8

6. ANFIS MODELLING AND VALIDATION

6.1 Input variable for ANFIS model development

This study utilizes three input variables for the ANFIS model: current, gas flow rate, and travel speed, with the relevant process parameters listed in Table 2. Tables 3 and 4 indicate results obtained from the current study. Results demonstrate that double-pass cladding with minimal current, gas flow rate, and travel speed yields superior properties due to improved filler deposition with the base alloy when compared with the other process parameters. However, correlating process parameters with material properties is often complex using traditional methods, highlighting the advantages of adopting the statistical learning model (ANFIS). ANFIS is particularly effective for developing predictive values.

6.2 ANFIS model for predicting the theoretical values

The ANFIS model was developed using samples fabricated according to the process parameters outlined in Table 3, with the goal of determining the tensile strength and microhardness values theoretically. This effective methodology excels in providing theoretical predictions for properties such as tensile strength and hardness. However, it can also be used to make various predictions of material properties as per the requirement. While ANFIS is part of the artificial neural networks (ANN) family, it offers flexible techniques for model development. Figure 9 and 10 depicts the ANFIS model schematic for samples with varying process parameters. Tables 5 and 6 show the RMSE and MAPE values for different membership functions, indicating that Gaussian functions yield the lowest error rates. Tables 7 and 8 list the experimental results along with the predicted tensile strength and microhardness values. For the purpose of the study, two decimals were considered for comparison with the experimental values for the predicted tensile and microhardness values. Due to the limited sample size, additional process parameters were assumed to improve validation and error measurement. For the ANFIS model development, the assumed process parameter conditions for the tensile and microhardness are listed in Tables 9 and 10. It is to be noted that the ANFIS model should be developed and tested for a large set of process parameters for better accuracy and improved efficiency in running the model. The data reveal minimal discrepancies between experimental results and predicted values for both cladding processes, affirming the ANFIS model's suitability for predicting tensile strength and microhardness. Each model generated 45 pairs of actual experimental outputs and ANFIS predictions using the leave-one-out cross-validation approach. The formula for calculating the predicted ANFIS values is provided in equation (1).

$$\text{Predicted Anfis TS} = \text{evalfis (UTS, Output);} \quad (1)$$

In fuzzy set theory, the membership function quantifies the degree of truth, ranging from 0 to 1, facilitating the resolution of ambiguous problems. These functions are typically depicted as curve-like shapes, each with specific names such as trimpf, pimf, gbellmf, gaussmf, and gauss2mf. Tables 5 and 6 display the RMSE and MAPE (%) values for each membership function evaluated in relation to the UTS plot in this study.

The membership function with the lowest RMSE and MAPE values is deemed the most reliable for ANFIS model development, providing predicted UTS values that closely align with experimental results. While other membership functions also yield predic–tions, their substantial variations and errors render them less applicable compared to the actual experimental data.

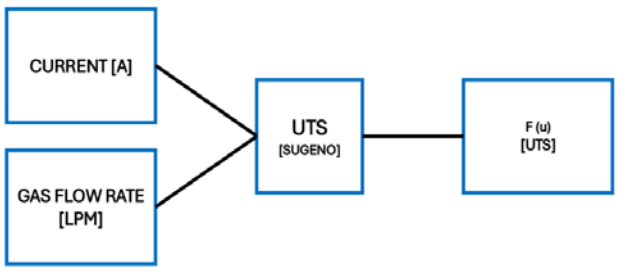

Figure 9: ANFIS Model Schematic for UTS

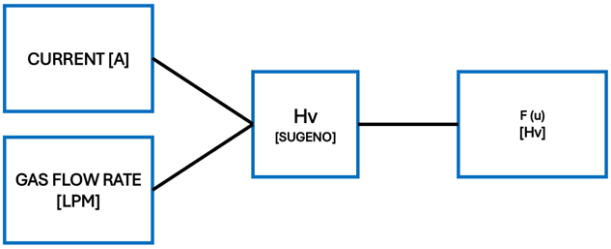

Figure 10: ANFIS Model Schematic for Microhardness

For each model, multiple pairs of actual experi–mental outputs and ANFIS-predicted outputs were ge–nerated using the leave-one-out cross-validation met–hod. The formula for calculating the predicted ANFIS values is provided in equation (2):

Predicted Anfis Hv = evalfis (Hv, Output); (2)

It is reported [41], that the employment of machine learning techniques can be an effective tool in a process. The present study lies in line with the literature for the prediction of values in a process.

Table 5. RSME Values for Different Membership function

Number of 'mf'			Type of Membership Function	RMSE (MPa)
Current	Gas Flow Rate	UTS		
2	2	2	trimf	55.3782
3	3	3	pimf	48.1246
3	4	3	pimf	51.3743
4	4	4	pimf	43.8417
3	2	3	gbellmf	59.8861
4	3	4	gaussmf	36.0936
5	5	5	gauss2mf	50.7295

Table 6. MAPE Values for Different Membership function

Number of 'mf'			Type of Membership Function	MAPE (%)
Current	Gas Flow Rate	UTS		
2	2	2	trimf	18.5428
3	3	3	pimf	24.7395
3	4	3	pimf	19.4266
4	4	4	pimf	18.2892
3	2	3	gbellmf	16.2977
4	3	4	gaussmf	12.9598
5	5	5	gauss2mf	16.0533

Table 7: Actual process parameters with experimental and predicted values

S. No	Current [A]	Flow rate [LPM]	Experimental UTS (MPa)	Predicted UTS (MPa)	Error percentage value
Sample 1	80	0.5	495.8	496.01	0.21
Sample 2	90	0.5	544.16	544.08	-0.08
Sample 3	100	1.0	527.37	527.02	-0.35
Sample 4	110	1.5	477.58	478.05	0.47
Sample 5	120	2.0	479.41	480.11	0.7
Sample 6	80	0.5	582.5	583.07	0.57
Sample 7	90	0.5	577.15	577.17	0.02
Sample 8	100	1.0	551.25	551.24	-0.01
Sample 9	110	1.5	505.67	506.31	0.64
Sample 10	120	2.0	576.74	577.20	0.46

Table 8: Actual process parameters with experimental and predicted values

S. No	Current [A]	Flow rate [LPM]	Experimental Microhardness (Hv)	Predicted Microhardness (Hv)	Error percentage value (%)
Sample 1	80	0.5	207.2	207.01	-0.19
Sample 2	90	0.5	216.3	216.09	-0.21
Sample 3	100	1.0	203.3	203.21	-0.09
Sample 4	110	1.5	200.8	201.25	0.45
Sample 5	120	2.0	189.6	190.17	0.57
Sample 6	80	0.5	220.5	221.01	0.51
Sample 7	90	0.5	204.6	204.9	0.3
Sample 8	100	1.0	209.4	210.02	0.62
Sample 9	110	1.5	214.1	214.15	0.05
Sample 10	120	2.0	210.8	211.13	0.33

Table 9: Assumed process parameters with predicted tensile values

S. No	Current [A]	Flow rate [LPM]	Predicted UTS (MPa)
1	90	0.7	556.6058
2	91	0.7	538.4992
3	92	0.7	462.9103
4	93	0.7	408.9715
5	94	0.7	484.4327
6	95	0.7	484.4762
7	96	0.7	486.4292
8	97	0.7	496.5588
9	98	0.7	517.9842
10	99	0.7	547.0114
11	100	0.7	563.2994
12	101	0.7	570.0724
13	102	0.7	573.9131
14	103	0.7	575.6863
15	104	0.7	576.3288
16	105	0.7	576.3571
17	106	0.7	576.1296
18	107	0.7	575.8839
19	108	0.7	575.7135
20	109	0.7	575.6176
21	110	0.7	576.5694
22	90	0.9	536.0395
23	91	0.9	535.1987
24	92	0.9	535.5223
25	93	0.9	536.1217
26	94	0.9	537.0661
27	95	0.9	538.2068
28	96	0.9	539.0813
29	97	0.9	539.1034
30	98	0.9	537.6964
31	99	0.9	534.0005
32	100	0.9	527.2894
33	101	0.9	511.2076
34	102	0.9	482.9873
35	103	0.9	433.8277
36	104	0.9	458.4889
37	105	0.9	453.9335
38	106	0.9	471.8928
39	107	0.9	502.5827
40	108	0.9	530.1557
41	109	0.9	537.568
42	110	0.9	552.8157
43	90	1.1	555.7394
44	91	1.1	543.2126
45	92	1.1	519.5573
46	93	1.1	474.9337
47	94	1.1	441.8669
48	95	1.1	435.1131
49	96	1.1	426.8115
50	97	1.1	467.2421
51	98	1.1	482.576
52	99	1.1	538.6816
53	100	1.1	551.0783
54	101	1.1	508.3019

55	102	1.1	485.9144
56	103	1.1	435.2287
57	104	1.1	421.787
58	105	1.1	431.871
59	106	1.1	456.5903
60	107	1.1	488.7415
61	108	1.1	523.9268
62	109	1.1	546.4554
63	110	1.1	558.3694

Table 10: Assumed process parameters with predicted microhardness values

S. No	Current [A]	Flow rate [LPM]	Predicted Hv
1	90	0.7	251.3297
2	91	0.7	249.9724
3	92	0.7	249.4157
4	93	0.7	248.6065
5	94	0.7	247.5413
6	95	0.7	246.3096
7	96	0.7	245.0842
8	97	0.7	244.0410
9	98	0.7	243.2781
10	99	0.7	242.8075
11	100	0.7	242.5998
12	101	0.7	242.6279
13	102	0.7	242.8845
14	103	0.7	243.3718
15	104	0.7	244.0702
16	105	0.7	244.9046
17	106	0.7	245.7492
18	107	0.7	246.4819
19	108	0.7	247.0394
20	109	0.7	247.4232
21	110	0.7	247.6698
22	90	0.9	248.0838
23	91	0.9	235.2333
24	92	0.9	229.4843
25	93	0.9	190.1938
26	94	0.9	217.4358
27	95	0.9	218.8976
28	96	0.9	208.1097
29	97	0.9	216.5002
30	98	0.9	225.4442
31	99	0.9	236.4606
32	100	0.9	240.0297
33	101	0.9	236.4493
34	102	0.9	225.4196
35	103	0.9	206.4584
36	104	0.9	180.0464
37	105	0.9	198.8089
38	106	0.9	217.3209
39	107	0.9	239.0551
40	108	0.9	248.3265
41	109	0.9	251.0618
42	110	0.9	253.9031
43	90	1.1	262.2697
44	91	1.1	252.7213
45	92	1.1	237.8482
46	93	1.1	216.2323
47	94	1.1	187.7928
48	95	1.1	154.9347
49	96	1.1	177.3083
50	97	1.1	194.6622
51	98	1.1	244.6994
52	99	1.1	232.8646
53	100	1.1	241.5673
54	101	1.1	216.3671
55	102	1.1	191.4174
56	103	1.1	189.0827
57	104	1.1	185.8530
58	105	1.1	183.2197
59	106	1.1	182.8511
60	107	1.1	198.5207
61	108	1.1	228.0400
62	109	1.1	231.4739
63	110	1.1	241.0997

7. MATERIAL PROPERTIES AND MACHINE LEARNING TECHNIQUE

The major objective of this study is to relate a strong relation between the actual material property of a fabri–cated sample and the machine learning technique, which is predominantly used for the theoretical prediction of values in a process. The complexity arises in how to relate these two different streams. Thus, we have add–ressed this with a novel approach to comparing the actual experimental data that we have procured during the process. The experimental data we have adopted in this study are metallurgical analysis, tensile, and micro–hardness values. In order to compare the experimental values that we have defined from the trial runs and as per the standard testing procedures, we need to have theoretical values of the same test methods that we have performed in this study. Therefore, as discussed, we have developed a model using the ANFIS model, considering the input parameters with a certain range of assumed process parameters. It is understood that machine learning techniques are highly efficient when they are tested with a larger number of working parameters. This is due to the fact that machine learning techniques are majorly working towards the collection of data in an application. The higher the data sets we use in an application, the more reliable outputs can be obtained from the trials we perform. However, it is well known that the material behavior of the alloy directly has a significant impact on the mechanical properties. It is studied from the obtained experimental values of the tensile and microhardness, which are directly proportional to the metallurgical behavior of the alloy. The refined and coarse grains had a significant effect on the mechanical properties. However, refined grains are achieved by adopting a feasible process parameter and a fabrication process that is much more easy and flexible to have control over during the cladding process. Thus, the actual experimental values and the predicted theoretical values, with the assistance of the ANFIS model, are in line with the data with the lowest error percentage values. Therefore, the ANFIS model can be widely used for the easy theoretical prediction of mechanical properties, and it can also be adopted for the optimal selection of process parameters. However, it is worth mentioning that the utilization of these machine-learning techniques in a process has to be chosen based on the requirements and needs of the industry.

8. CONCLUSIONS

The following observations are concluded from the present work:

1. Successful single and double pass cladding of SS 304 fillers is carried on SS 316 L base alloy.
2. A metallurgical survey was performed for the samples across different zones.
3. Refined grain structures resulted in enhanced material properties.
4. The increase in the tensile and microhardness values is observed as 13.2 % and 42.5 % from the experimental outputs.
5. Double-pass cladding has shown improved output compared to single-pass cladding due to better filler deposition over the base alloy.
6. A novel approach has been attempted to relate the material properties and machine learning techniques.
7. The ANFIS model was developed for the trials, and the theoretical values were predicted to be the same.
8. The experimental and theoretical values are reliable, with the lowest error percentage.
9. Machine learning techniques could effectively be used to predict optimal process parameters in a feasible manner compared with other existing traditional techniques.

ACKNOWLEDGMENT

The authors sincerely thank **Mr. Pradeep Krishna R**, Design Engineer, Aptiv Connection Systems, India. For his consistent support in the preparation of machine learning data for the manuscript.

REFERENCES

[1] Kuang-Hung Tseng, Chih-Yu Hsu, Performance of activated TIG process in austenitic stainless steel welds, Journal of Materials Processing Technology, 211, 2011, 503–512.

[2] K. H. Tseng, C. P. Chou, Effect of pulsed gas tungsten arc welding on angular distortion in austenitic stainless steel weldments, Science and Technology of Welding and Joining, 2001, Vol. 6 No. 3, 149–153.

[3] K. H. Tseng, C. P. Chou, Effect of nitrogen addition to shielding gas o residual stress of stainless steel weldments, Science and Technology of Welding and Joining, 2001, Vol. 7 No. 1, 57–62.

[4] K. H. Tseng, C. P. Chou, The effect of pulsed GTA Welding on the residual stress of a stainless steel weldment, Journal of Material Processing Technology, 123, 2002, 346 – 353.

[5] V. Shankar, T.P.S. Gill, S.L. Mannan, S. Sundaresan, Solidification Cracking In Austenitic Stainless Steel Welds, Sadhana Vol. 28, Parts 3 & 4, 2003, 359 – 382.

[6] M. Brandt, S. Sun, N. Alam, P. Bendeich, A. Bishop, Laser cladding repair of turbine blades in power plants: from research to commercialisation, International Heat Treatment and Surface Engineering, 2009, VOL 3 NO 3, 105 – 114.

[7] E. Capello, D. Colombo, B. Previtali, Repairing of sintered tools using laser cladding by wire, Journal of Materials Processing Technology, 164–165, 2005, 990 – 1000.

[8] Ferenc Gillemot, Overview of reactor pressure vessel cladding, Int. J. Nuclear Knowledge Management, Vol. 4, No. 4, 2010, 265 – 278.

[9] Jun Yan, Ming Gao, Xiaoyan Zeng, Study on microstructure and mechanical properties of 304 stainless steel joints by TIG, laser and laser-TIG hybrid welding, Optics and Lasers in Engineering, 48, 2010, 512 – 517.

[10] H.M. Soltani, M. Tayebi, Comparative study of AISI 304L to AISI 316L stainless steels joints by TIG and Nd: YAG laser welding, Journal of Alloys and Compounds (2018), doi:10.1016/j.jallcom.2018.06.302.

[11] N. Kumar, M. Mukherjee, A. Bandyopadhyay, Comparative study of pulsed Nd: YAG laser welding of AISI304 and AISI316 stainless steels, Optics & Laser Technology, 88, 2017, 24 – 39.

[12] S. Chen, M. Zhang, J. Huang, C. Cui, H. Zhang, X. Zhao, Microstructures and mechanical property of laser butt welding of titanium alloy to stainless steel, Materials and Design, Vol 53, 2014, 504 – 511.

[13] L.D. Scintilla, L. Tricarico, M. Brandizzi, A.A. Satriano, Nd:YAG laser weldability and mechanical properties of AZ31 magnesium alloy butt joints, Journal of Materials Processing Technology, Vol 210, 2010, 2206 – 2214.

[14] A. Behera, Optimization of process parameters in laser welding of dis-similar materials, Materials Today: Proceedings, 2214 – 7853.

[15] J.D. Linton, Q. Jiang, C.J. Gatti, M.J. Embrechts, Erratum for "Anawa, E.M. and Olabi, A.G. Using Taguchi method to optimize welding pool of dissimilar Laser Welded Components", Optics and Laser Technology, 2008, 40 (2), 379 – 388.

[16] Y. Huang, X. Gao, B. Ma, G. Liu, Nanfeng Zhang, Yanxi Zhang, Deyong You, Optimization of weld strength for laser welding of steel to PMMA using Taguchi design method, Optics and Laser Technology, 2020, 0030-3992.

[17] A. Khajanchee, S.K. Pradhan, P. Jain, Experimental Investigations To Optimize Process Parameters For CO2 Laser Welded Alloy Steel Automotive Gears, Materials Today: Proceedings 5, 2018, 11636 – 11654.

[18] K.Y. Benyounis, A.G. Olabi, M.S.J. Hashmi, Multi-response optimization of CO2 laser-welding process of austenitic stainless steel, Optics & Laser Technology, Vol 40, 2008, 76 – 87.

[19] V. Gunaraj, N. Murugan, Application of response surface methodology for predicting weld bead quality in submerged arc welding of pipes, Journal of Materials Processing Technology, Vol 88, 1999, 266 – 275.

[20] M.M.A. Khan, L. Romoli, M. Fiaschi, G. Dini, F. Sarri, Experimental design approach to the process

parameter optimization for laser welding of martensitic stainless steels in a constrained overlap configuration, Optics & Laser Technology, Vol 43, 2011, 158 – 172.

[21] X. Cao, Z. Li, X. Zhou, Z. Luo, J. Duan, Modeling and optimization of resistance spot welded aluminum to Al-Si coated boron steel using response surface methodology and genetic algorithm, Measurement, Vol 171, 2021, 108766.

[22] J. Long, W. Huang, J. Xiang, Q. Guan, Z. Ma, Parameter optimization of laser welding of steel to Al with pre-placed metal powders using the Taguchi-response surface method, Optics and Laser Technology, Vol 108, 2018, 97 – 106.

[23] P. Sathiya, K. Panneerselvam, M.Y. Abdul Jaleel, Optimization of laser welding process parameters for super austenitic stainless steel using artificial neural networks and genetic algorithm, Materials and Design, Vol 36, 2012, 490 – 498.

[24] Y. Whan Park, S. Rhee, Process modeling and parameter optimization using neural network and genetic algorithms for aluminum laser welding automation, Int J Adv Manuf Technol, 2008, Vol 37, 1014 – 1021.

[25] Y.K. Liu, Y.M. Zhang, Iterative Local ANFIS-Based Human Welder Intelligence Modeling and Control in Pipe GTAW Process: A Data-Driven Approach, IEEE/ASME Transactions on Mechatronics, Vol. 20, No. 3, 2015, 1079 – 1088.

[26] Y. M. Zhang, R. Kovacevic, L. Li, Characterization and Real-time Measurement of Geometrical Appearance of the Weld Pool, Int. J. Mach. Tools Manufact., Vol 36, No. 7, 1996, 799 - 816.

[27] D.S. Correia et al., Comparison between genetic algorithms and response surface metho–dology in GMAW welding optimization, Journal of Materials Processing Technology, Vol 160, 2005, 70 – 76.

[28] X. Ma, Z. Sun, P. Cui, J. Wu, Optimization of the welding process parameters of Mg–5Gd–3Y magnesium alloy plates with a hybrid Kriging and particle swarm optimization algorithm, Proc IMechE Part C: J Mechanical Engineering Science, 2017.

[29] Y. Ai, X. Shao, P. Jiang, P. Li, Y. Liu, W. Liu, Welded joints integrity analysis and optimization for fiber laser welding of dissimilar materials, Optics and Lasers in Engineering, Vol 86, 2016, 62 – 74.

[30] D. Katherasan, Jiju V. Elias, P. Sathiya, A. Noorul Haq, Simulation and parameter optimization of flux cored arc welding using artificial neural network and particle swarm optimization algorithm, J Intell Manuf, Vol 25, 2014, 67 – 76.

[31] M. Ťavodová, N. Náprstková, M. Hnilicová, P. Beňo, Quality Evaluation of Welding Joints by Different Methods, FME Transactions, 2020, Vol 48, 816 – 824.

[32] H. Vemaaboina, S. Akella, R.K. Buddu, Distortion Control in Laser Beam Welding using Taguchi ANOVA Analysis, FME Transactions, Vol 48, 2020, 180 – 186.

[33] A. Lukianenko, T.M. Labur, A.G. Pokliatskyi, S. Motrunich, D. Bajic, Investigation of Fatigue Strength and Norms of Emission of Harmful Substances in the Air during MIG and TIG Welding of 1460 Aluminium - Lithium Alloy, FME Transactions, 2019, 47, 608 – 612.

[34] K. Andersen, G.E. Cook, G. Karsai, K. Ramaswamy, Artificial Neural Networks Applied to Arc Welding Process Modeling and Control, IEEE Transactions on Industry Applications, Vol. 26, No. 5, 1990, 824 – 830.

[35] Z. Yuguang, X. Kai, S. Dongyan, An improved artificial neural network for laser welding parameter selection and prediction, Int J Adv Manuf Technol, 2013, Vol 68, 755 – 762.

[36] S. Ghosal, S. Chaki, Estimation and optimization of depth of penetration in hybrid CO2 LASER-MIG welding using ANN-optimization hybrid model, Int J Adv Manuf Technol, 2010, Vol 47, 1149 – 1157.

[37] A. Sanchez Roca, H. C. Fals, J. B. Fernandez, E. J. Macias, M. P. de la Parte, Artificial neural networks and acoustic emission applied to stability analysis in gas metal arc welding, Science and Technology of Welding and Joining, 2009, Vol 14, No 2, 117 – 124.

[38] M.-J. Tsai, C.-H. Li, C.-C. Chen, Optimal laser-cutting parameters for QFN packages by utilizing artificial neural networks and genetic algorithm, Journal of Materials Processing Technology, Vol 208, 2008, 270 – 283.

[39] H. Inoue, T. Koseki, M. Fuji, Epitaxial growth and phase transformation of austenitic stainless steel weld metals near fusion boundaries: Study of solidification and transformation of Cr-Ni stainless steel weld metals, Welding International, 1998, 195-206.

[40] J.C. Lippold, D.J. Kotecki, Welding metallurgy and weldability of stainless steels, Wiley, 2005.

[41] V. Kumar A., P. Krishna R., M.F. Hasanabadi, Sathickbasha K., Evaluation of Machine Learning Techniques for the Nd: YAG Laser & TIG Welded Stainless Steel 304, FME Transactions, 2024, 52, 90-102.

[42] V. Kumar A., P. Krishna R., E. Taban, Enhancement of Material Properties of SS 316L Base Metal by TIG Cladding Process, Journal of Alloys and Metallurgical Systems, 2024, https://doi.org/10.1016/j.jalmes.2024.100121

КОРЕЛАЦИЈА СВОЈСТАВА МАТЕРИЈАЛА И ТЕХНИКА МАШИНСКОГ УЧЕЊА НА ТИГ ОБЛОЖЕНОЈ SS 316L ОСНОВНОЈ ЛЕГУРИ СА SS 304 ДОДАТНИМ МАТЕРИЈАЛОМ

А.В. Кумар, К.Р.Ш. Вавиву, К. Сатикбаша

Облога од волфрама за заваривање са инертним заштитним гасом (ТИГ) је најперспективнија и најизводљивија техника усвојена за заваривање

легура од нерђајућег челика. У овом раду, SS 304 пунила су нанесена преко SS 316L кроз ТИГ процес облагања и проучавано је понашање легуре. Оптичке студије, вредности затезања и микро–тврдоће ТИГ обложеног основног метала од SS 316L са SS 304 материјалом за пуњење су у корелацији са техником машинског учења. Модел Adaptive Neuro-Fuzzi Inference Systems (АНФИС) је коришћен у овој студији да се теоретски предвиде вредности. Показало се да се корелација између експери–менталних вредности и теоријских вредности добро слаже. Утврђено је да је побољшање механичких својстава легуре SS 316L обложене ТИГ-ом солидније и поузданије него код легуре CC 316L на бази. Одговарајући избор параметара процеса и врсте облоге (једноструки или двопролазни) значајно су утицали на побољшање својстава мате–ријала у већој мери. Из експерименталних резултата утврђено је повећање вредности затезања и микро–тврдоће за 13,2 % и 42,5 %. Међутим, доступан је широк спектар методологија/техника за теоријско предвиђање вредности, док је техника машинског учења имала значајан утицај на поуздано пред–виђање вредности. Стога је утврђено да усвајање техника машинског учења може помоћи флекси–билно у идентификацији поузданог и оптималног параметра процеса у процесу производње.